



LUND UNIVERSITY

State Estimation in Power Networks II

Comparison of Methods

van Overbeek, A. J. M.

1974

Document Version:

Publisher's PDF, also known as Version of record

[Link to publication](#)

Citation for published version (APA):

van Overbeek, A. J. M. (1974). *State Estimation in Power Networks II: Comparison of Methods*. (Research Reports TFRT-3112). Department of Automatic Control, Lund Institute of Technology (LTH).

Total number of authors:

1

General rights

Unless other specific re-use rights are stated the following general rights apply:

Copyright and moral rights for the publications made accessible in the public portal are retained by the authors and/or other copyright owners and it is a condition of accessing publications that users recognise and abide by the legal requirements associated with these rights.

- Users may download and print one copy of any publication from the public portal for the purpose of private study or research.
- You may not further distribute the material or use it for any profit-making activity or commercial gain
- You may freely distribute the URL identifying the publication in the public portal

Read more about Creative commons licenses: <https://creativecommons.org/licenses/>

Take down policy

If you believe that this document breaches copyright please contact us providing details, and we will remove access to the work immediately and investigate your claim.

LUND UNIVERSITY

PO Box 117
221 00 Lund
+46 46-222 00 00

TFRT-3112

STATE ESTIMATION IN POWER NETWORKS II
Comparison of methods

A.J.M. van Overbeck

Report 7403(C) April 1974
Lund Institute of Technology
Division of Automatic Control

TILLHÖR REFERENSBIBLIOTEKET
UTLÄNAS EJ

ERRATA A.J.M. van Overbeek: State Estimation in Power
Networks II, Comparison of methods.

<u>page</u>	<u>line</u>	<u>column</u>		<u>read</u>
4	6+	right	$G^T(\underline{x}_i)$	$G^T(\underline{\hat{x}}_i)$
8	5+	right	much	many
19	6+		both ends	one end
27	4-	right	04	0.4

STATE ESTIMATION IN POWER NETWORKS II

Comparison of methods

A.J.M. van Overbeek

ABSTRACT

The results of a comparison of three different state estimation methods are presented. These methods are a version of the weighted least squares estimator of F.C. Schweppe, the method developed by Systems Control, Inc. and the lineflow method in use with the American Electric Power Service Corporation. All methods are tested on the same network using the same measurements. The method of Systems Control turned out to be best because it exploits the slowly changing state. The other two methods do not use the information contained in the old estimate. An other conclusion is that the choice of busvoltages as state variables is doubtful since the power flow in the network is determined by the differences between the nearly equal busvoltages.

Contents.

	Page
1. Introduction.	3
2. The three methods chosen for comparison.	4
3. Set up of the comparison.	8
3.1 The CIGRE-network and its properties.	8
3.2 The organization of the simulation.	16
3.3 Measurement systems.	19
3.4 Load patterns.	19
3.5 Test quantities.	21
4. The properties of the three methods.	23
4.1 Method A.	23
4.2 Method B.	25
4.2.1 Tuning of ordering of measurements.	25
4.2.2 Tuning of Q.	27
4.3 Method C.	28
5. The results of the comparison.	30
5.1 Computing time and storage.	30
5.2 The simulations.	32
5.3 Interpretation of the results.	37
6. Conclusions and suggestions.	38
7. Acknowledgements.	40
8. References.	41
 Appendix: The simulations.	 43

1. Introduction.

In a previous report /1/* a literature survey was given on state estimation methods in power networks. A distinction was made between methods using the information that the state does not change too much between two timepoints and methods that do not use this information. Three methods were presented for further comparison. In this report the results of this comparison are presented. In a companion report /2/ the programs developed for this comparison are described.

The three chosen methods are: a version of the weighted least squares estimator of F.C.Schwepe (method A), the method developed by Systems Control, Inc and the Bonneville Power Administration (method B) and finally the lineflow method in use with the American Electric Power Service Corp. (method C). In the remainder of this report these methods will be referred to as method A, B and C respectively.

The next chapter gives a description of these three methods. The power network used for simulation and the chosen test quantities for comparison and the simulation in general are the subject of chapter 3. In chapter 4 the properties of the three methods are described. The comparison proper is the subject of chapter 5, followed by the conclusions in chapter 6. All methods are tested on the same network and use the same measurements. The comparison is not at all complete. What happens when e.g. the measurements have bias, one or a few measurements are in gross error, or the estimators use wrong network parameters or an incorrect network structure, is not investigated.

* See chapter 8: references

2. The three methods chosen for comparison.

The first method, method A, is a version of the weighted least squares estimator of F.C. Schweppe /3, 4/.

The estimate at timepoint $k + 1$ can be determined in an iterative way:

$$\underline{x}_{i+1} = \underline{x}_i + [G^T(\underline{x}_1)R^{-1}G(\underline{x}_1)]^{-1}G^T(\underline{x}_i)R^{-1}\{\underline{y} - g(\underline{x}_{k,i})\} \quad (2-1)$$

with

- \underline{x}_i the estimate after iteration i .
- $G(\underline{x}_1)$ the jacobian evaluated at the last linearization point: \underline{x}_1 .
- R^{-1} diagonal weighting matrix (covariance matrix) of measurement errors.
- \underline{y} the measurement vector at $t = k + 1$.
- $g(\underline{x}_{k,i})$ the measurement function based on the estimate after i iterations.

$$\underline{x}_{k+1,0} = \underline{x}_k$$

Under normal operation one iteration is sufficient to obtain a new estimate, but for start up purposes more iterations are necessary. Where and how often $G(\underline{x}_1)$ is computed is treated in chapter 4.

The second method, method B, uses sequential processing of measurements with relinearization after each measurement /4, 5, 6/. At $t = k + 1$ the estimate after processing the $j + 1$ -st measurement is given by:

$$\begin{aligned} \underline{x}_{j+1} &= \underline{x}_j + K_{j+1} \{y_{j+1} - g_{j+1}(\underline{x}_j)\} \\ K_{j+1} &= P_j G_{j+1}^T(\underline{x}_j) [G_{j+1}(\underline{x}_j) P_j G_{j+1}^T(\underline{x}_j) + R_{j+1}]^{-1} \quad (2-2) \\ P_{j+1} &= P_j - \text{diag}[K_{j+1} G_{j+1}(\underline{x}_j) P_j] \\ P_0 &= P_k + Q \end{aligned}$$

with \underline{x}_{j+1} the estimate after processing $j + 1$ measurements.

y_{j+1} the $j + 1$ -st measurement.

g_{j+1} the $j + 1$ -st measurement function

G_{j+1} the jacobian row associated with the $j + 1$ -st measurement.

P_j the diagonal covariance matrix after processing j measurements.

R_{j+1}^{-1} the weighting factor for the $j + 1$ -st measurement.

Q diagonal matrix to be added to P indicating how much weight should be placed on the old estimate.

Also here more iterations are possible, but usually one iteration is sufficient, even for startup (see chapter 4).

The last method, method C, first computes the linevoltages from lineflow measurements and considers these as new measurement variables /7, 8, 9, 10/. The relationship between the line and busvoltages is linear and only dependent on network structure. Since the new measurement variables are dependent on the state (the power needed for charging the line is dependent on the bus-voltage) the estimate has to be obtained in an iterative way. The linevoltage j in iteration $i + 1$ at $t = k + 1$ is computed from the j -th lineflow measurement as:

$$z_j = Z_{ab,j} \left\{ \frac{y_j^*}{x_{i,j}^*} + Y_{aa,j} x_{i,j} \right\} \quad (2-3)$$

with z_j the j -th linevoltage.

$Z_{ab,j}$ the series impedance of the line concerned.

y_j the complex lineflow measurement.

$x_{i,j}$ the busvoltage at the line-end concerned.

$Y_{aa,j}$ the shunt admittance at the line-end concerned.

* denotes complex conjugate.

The linear relationship between the new measurement variables \underline{z} and the state variables \underline{x} is given by:

$$\underline{z} = A\underline{x} + \underline{e} = B\underline{E} + A_g E_g + \underline{e} \quad (2-4)$$

with \underline{e} measurement error.

E_g reference voltage.

A_g matrix column of A associated with reference voltage.

B matrix A minus column A_g .

\underline{E} busvoltages minus reference voltage.

The new estimate is obtained as:

$$\hat{E}_{i+1} = [B^T D B]^{-1} \{Z_{k+1} - A_g E_g\}$$

$$\underline{\hat{x}}_{i+1} = \begin{bmatrix} \hat{E}_{i+1} \\ E_g \end{bmatrix} \quad (2.5)$$

with D diagonal matrix of linevoltage weighting factors computed from the lineflow weighting factors as

$$D_{jj} = \frac{W_{jj}}{|Z_{ab,j}|^2}$$

and $\underline{\hat{x}}_0 = \underline{\hat{x}}_k$

Methods A and C do not use information from older measurements but only the information contained in the new measurement set, while method B may be seen as averaging over more than one measurement set.

3. Set up of the comparison.

The first part of this chapter is devoted to the treatment of the CIGRE power network used to test the three methods, and its properties. These characteristics, common to many power networks, are responsible for much of the properties of the different estimation methods. The latter part of this chapter treats the simulation proper: the test quantities, the different measurement systems, measurement accuracies and load patterns chosen for simulation.

3.1 The CIGRE-network and its properties.

The power network used for simulation is the CIGRE network, consisting of 10 buses and 13 lines. It was chosen because of its reasonable size and because it is known from economic load dispatch studies. Fig. 3-1 shows the network with the bus, line and generator numbers.

These numbers are used throughout the simulation.

The two ends of each line are marked A and B respectively.

All calculations are done in the per unit system with a base voltage of 220 kV and a base power of 100 MVA. Table 3-1 gives the network parameters in per unit values. All lines are modelled as π -sections with equal purely capacitive shunt admittances.

10 BUSES
13 LINES
14 GENERATORS

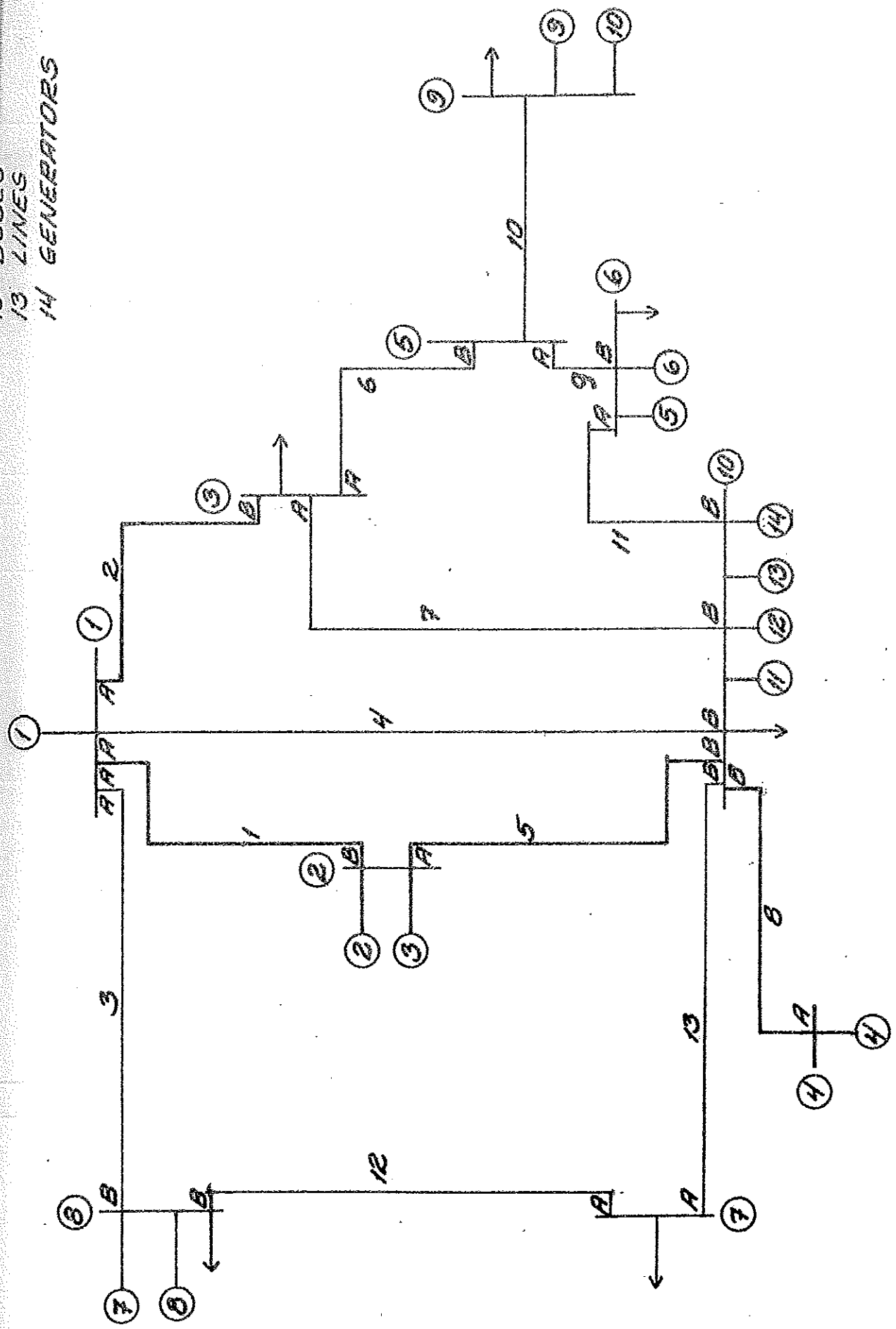


Fig. 3.1

CIGRE NETWORK WITH BUS AND LINE AND GENERATOR NUMBERS

Line	Aend	Bend	Shunt capaci- tance at both line ends	Real part of series imped.	Imag. part of series imp.
1	1	2	0.09680	0.01033	0.05062
2	1	3	0.09680	0.01188	0.05785
3	1	8	0.09680	0.04711	0.12934
4	1	10	0.14520	0.01240	0.08161
5	2	10	0.04840	0.01033	0.05062
6	3	5	0.09680	0.05103	0.20041
7	3	10	0.09680	0.05103	0.20041
8	4	10	0.09680	0.00413	0.02066
9	5	6	0.09680	0.01963	0.06570
10	5	9	0.14520	0.01240	0.08161
11	6	10	0.04840	0.00775	0.05114
12	7	8	0.14520	0.01705	0.06674
13	7	10	0.14520	0.01705	0.06818

Table 3-1: The network parameters.

Table 3-2 gives the generator parameters in per unit values:

The minimum and maximum generated active power for each generator plus the coefficients a_1 and a_2 of the generator cost function

$$a_1 P_{gen} + a_2 P_{gen}^2$$

These coefficients are used in a load dispatch. The reactive generator limits are not used in the simulation and therefore not included. For more details on the use of the generator data, see the next section.

Generator	minimum active power	maximum active power	a_1	a_2
1	0.8	2.17	0.773	0.340
2	0.8	2.17	0.395	0.443
3	0.8	2.17	0.538	0.407
4	0.8	2.17	0.489	0.393
5	0.4	1.08	0.675	1.033
6	0.4	1.08	0.803	0.966
7	0.8	2.17	0.394	0.392
8	0.4	1.08	1.367	0.623
9	0.3	0.72	1.513	0.602
10	0.4	1.08	0.678	0.773
11	0.8	2.17	0.768	0.350
12	0.8	2.17	0.623	0.384
13	0.4	1.08	0.636	1.008
14	0.4	1.08	0.696	0.978

Table 3-2: Generator data.

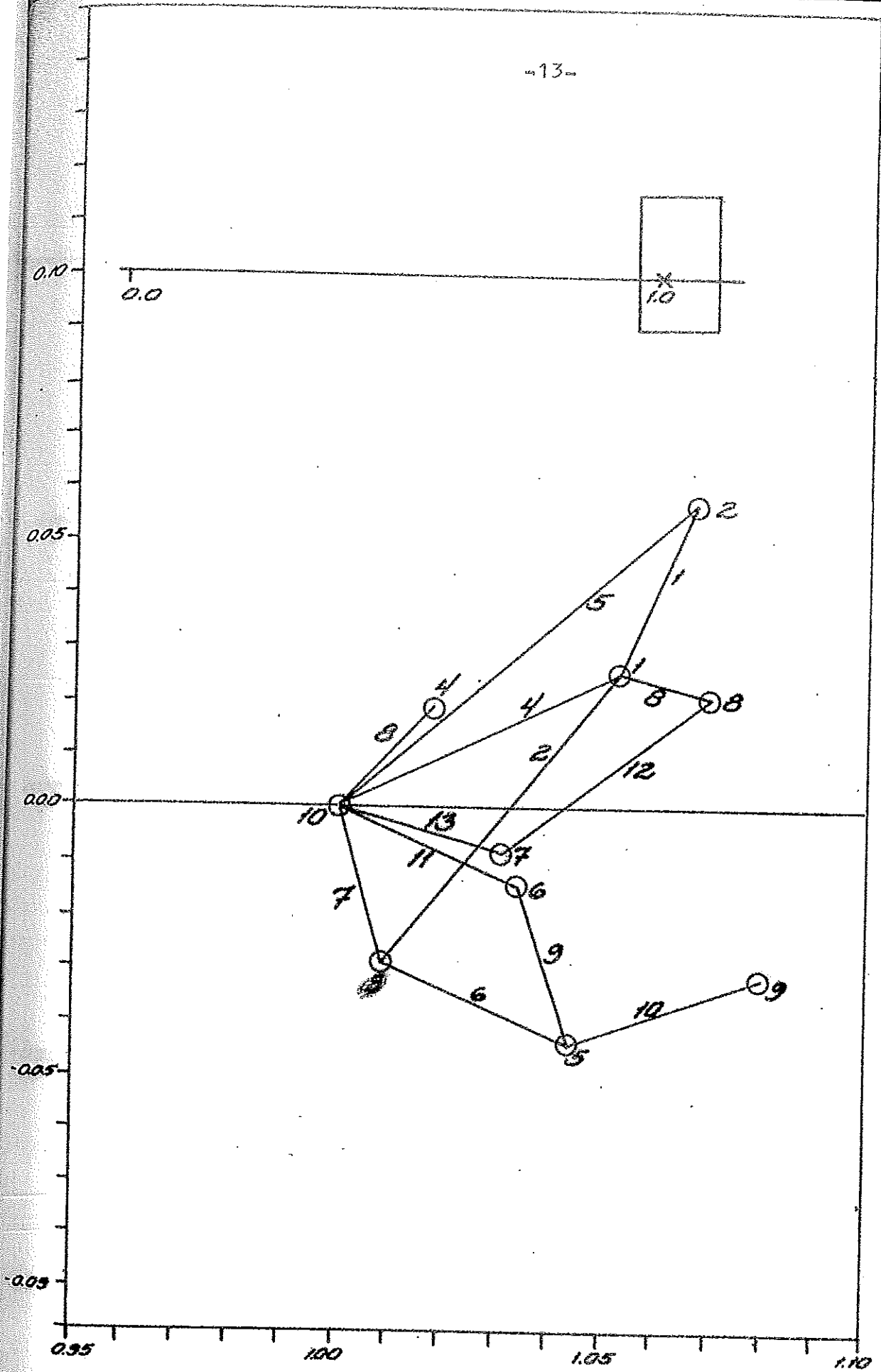
The minimum and maximum active and reactive loads are given in table 3-3. Buses 1, 2 and 4 have no load.

Bus	minimum active load	minimum reactive load	maximum active load	maximum reactive load
3	1.2	0.90	2.6	1.70
5	0.6	0.30	1.5	0.75
6	0.6	0.20	1.0	0.35
7	0.6	0.25	1.1	0.55
8	1.0	0.60	2.5	1.70
9	0.5	0.15	1.0	0.35
10	5.1	3.10	10.0	6.30

Table 3-3: Load data.

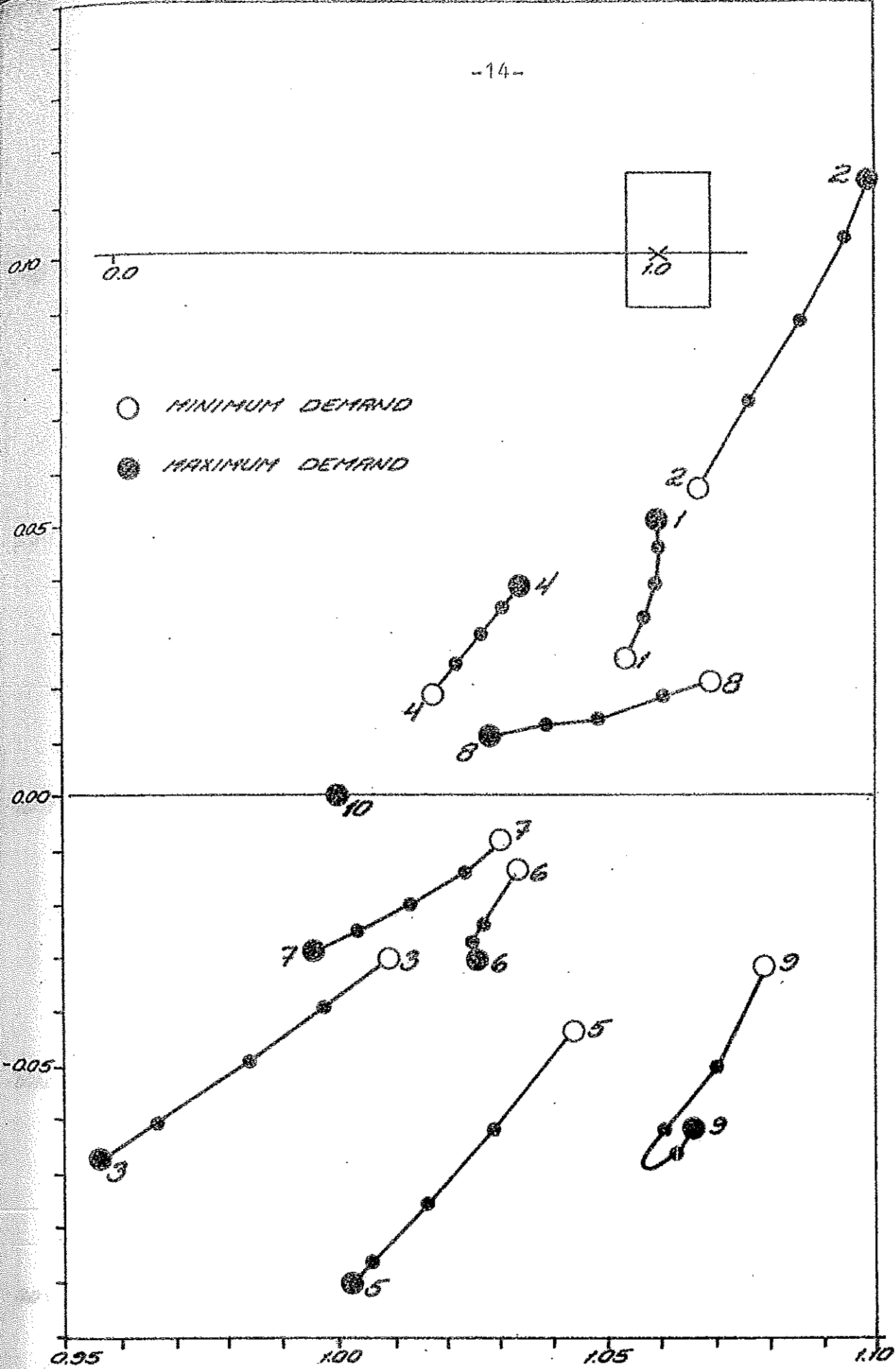
Heavy load buses are buses 10, 8 and 3. Buses 10, 2 and 8 have the most generating power available. Lines 1, 2, 5 and 8 turned out to be the most heavily loaded lines. These are drawn with thick lines in fig. 3.1.

The powerflow in a power network is determined by the busvoltages. The positions of the busvoltages at minimum demand is given in fig. 3.2. Note that all busvoltages lie very close together. In the top half is drawn on scale the distance of the picture to zero. The powerflow in each line is mainly determined by the voltage difference across the line. These linevoltages are also drawn in fig. 3.2. Since the powerflow mainly is determined by the voltage differences, it is necessary to know the busvoltages with a larger relative accuracy than the linevoltages. Fig. 3.3 show how the bus-voltages move when the load demand changes from minimum to maximum. The assumption is made that all demands rise at the same constant rate.



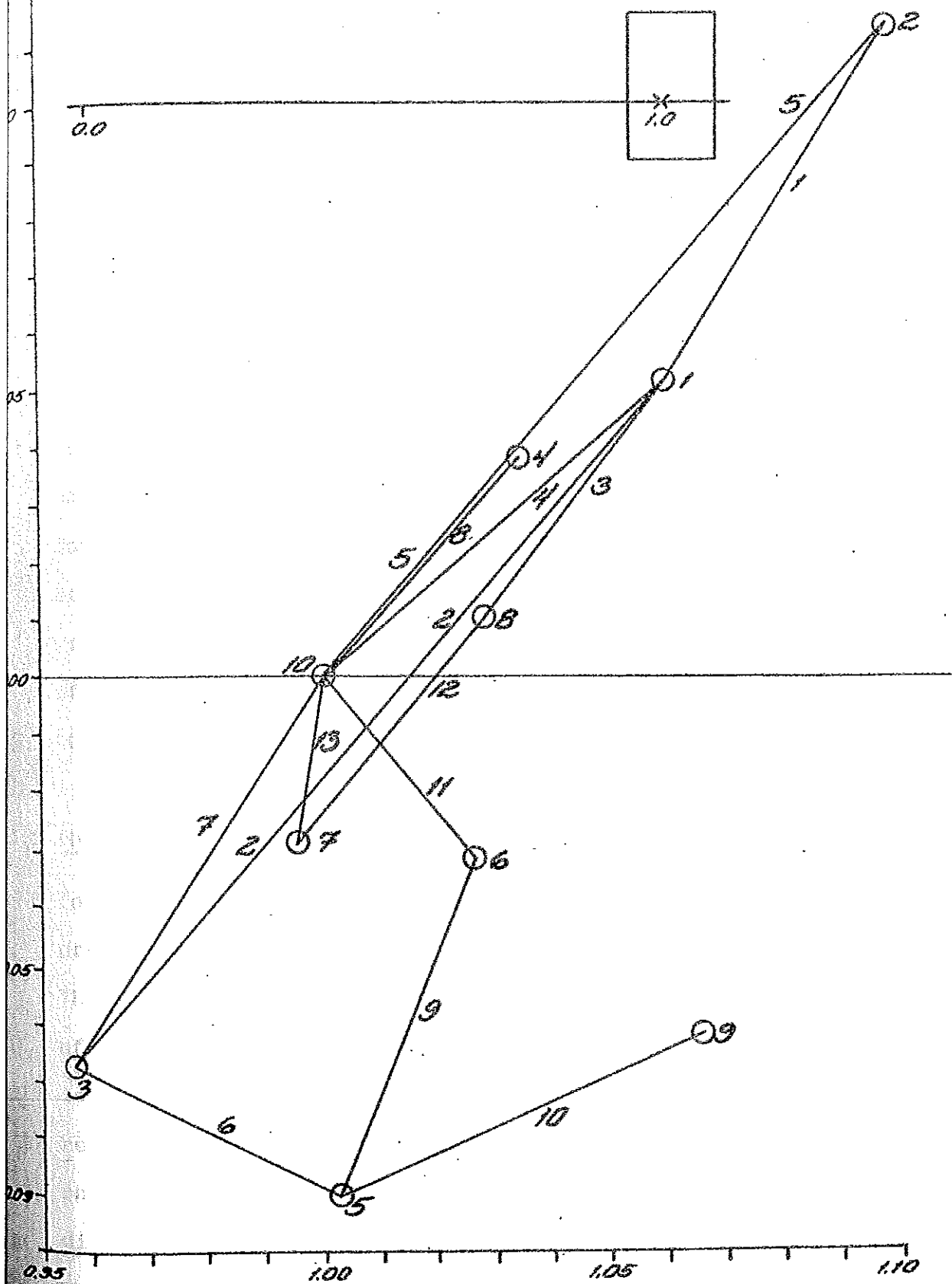
BUS AND LINE VOLTAGES AT MINIMUM DEMAND

Fig. 3.2



BUS VOLTAGES AS FUNCTION OF THE DEMAND

fig. 3.3



BUS AND LINE VOLTAGES AT MAXIMUM DEMAND

Fig. 3.4

Note that the busvoltages change faster in the beginning than at the end of the load rise. The bus and linevoltages at maximum demand are shown in fig. 3.4. Note the linevoltages associated with the heavy loaded lines 1, 2 and 5.

What the methods try to do is to estimate a number of nearly equal busvoltages while the powerflow in the network is determined by the differences between the busvoltages. This is valid for this and many powernetworks in practice but not for powernetworks with very long highly loaded lines and therefore large angle differences between busvoltages. A consequence of this property is that the powerflow in the network does not change very much when the whole structure of linevoltages moves along the real axis in fig. 3.2 or 3.4. Only the currents through the shunt admittances will be affected and these are relatively small compared with the currents through the series impedances.

3.2 The organization of the simulation.

To compare the three methods a total of 41 subroutines and 4 main programs were written.

These are described in /2/. Fig. 3.5 gives a simplified flowdiagram of the main simulation program. At each timepoint the true state is computed from the power demand because this is closest to reality. First the total active demand is divided over the generators by an economic load dispatch neglecting line losses. This dispatch needs the generator characteristics of table 3-2. The reactive demand is divided over the generators in the same ratio as the active demand.

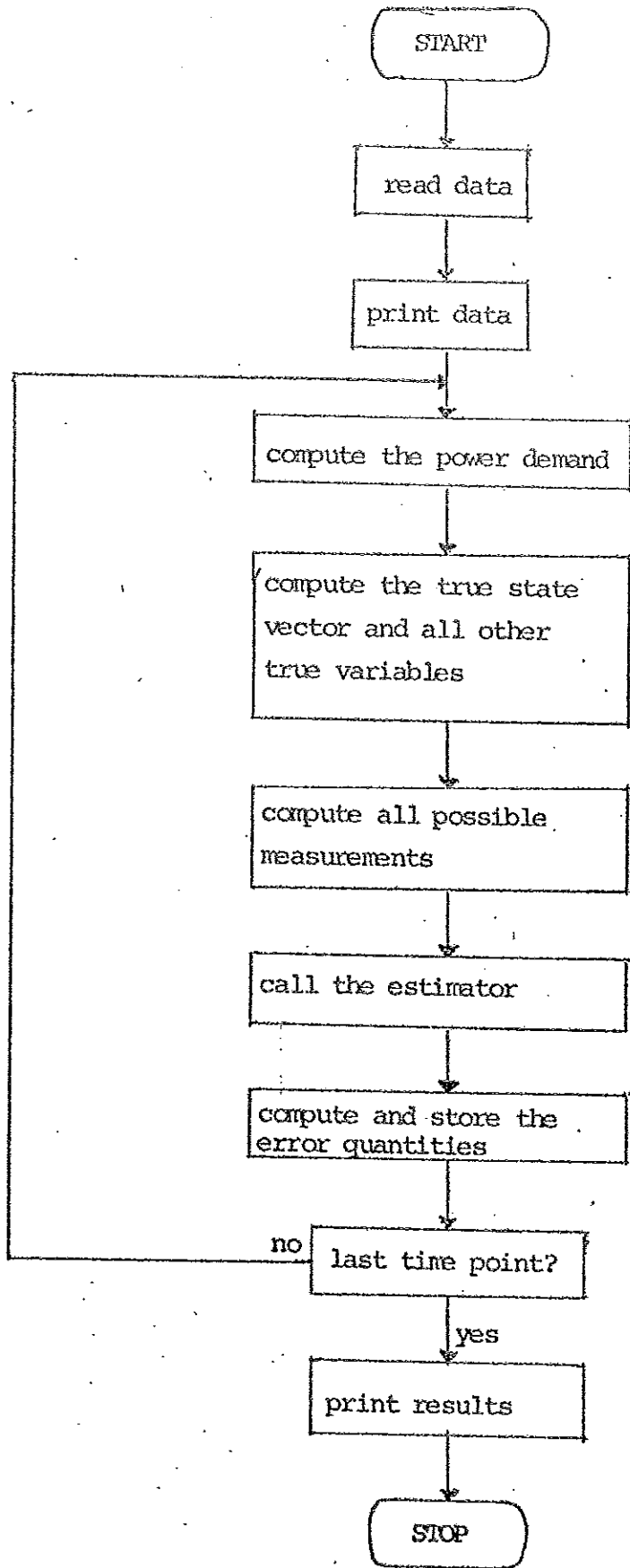


Fig. 3.5 Mainprogram used for simulation.

This means that all generators are operated at the same cos ϕ . Now the bus injections can be computed in order to do a conventional Newton-Raphson load flow to compute the true state. Bus 10 is chosen as slack bus since this bus has the largest generating capacity. From the true state the measurements are computed by adding measurement noise. The measurement noise is modelled as $\alpha \times \text{full scale} + \beta \times \text{true value}$. The measurements used in the comparison are voltage, active and reactive lineflow measurements. The full scale values for these measurements are given in the following table:

Voltage measurements.

All full scale values: 1.0

Active and reactive lineflow measurements on both ends of a line.

line	full scale value
1	5.0
2	5.0
3	1.0
4	2.0
5	5.0
6	1.0
7	1.0
8	5.0
9	2.0
10	2.0
11	2.0
12	1.0
13	1.0

Table 3-4: Full scale values.

3.3 Measurement systems.

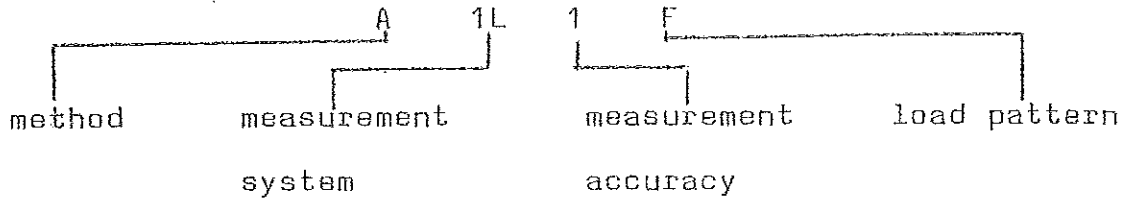
To compare the influence of the choice of measurement system three different ones were chosen: one voltage measurement at the reference bus (bus 10) and all lineflow measurements on both ends of each line, one voltage measurement at bus 10 and all lineflow measurements on both ends of each line and finally all voltage measurements and all lineflow measurements on one end of each line. The former two are used with all three methods while the latter one is used only with method A and B. This is done to check how these methods behaved when using a different measurement system as necessary for method C. The influence of measurement accuracy was tested by choosing both α and β 0.01 and 0.05 respectively. The value 0.05 is very bad compared to reality. This value was chosen to test the influence of a larger redundancy compared to a larger accuracy. 0.01 is much more realistic.

3.4 Load patterns.

As said before the true state is calculated from the load demand at each timepoint. Each simulation lasts 360 timepoints. If the sampling interval is set to 20 secs this means a total time of two hours.

Three load patterns were used: a constant one to test the estimators under quiet operation, a step change in all loads from minimum to maximum at timepoint 180 to test the estimators on their ability to follow a sudden change and finally a ramp to imitate the load rise during the early morning hours. In the simulation the loads on all buses rise at the same rate from minimum to maximum in one hour (timepoint 91-270).

The simulations are named after the following conventions.



measurement system:

- 1L busvoltage at bus 10 plus active and reactive lineflow at one end of each line.
- LV all busvoltages plus active and reactive lineflow at one end of each line.
- 2L busvoltage at bus 10 plus active and reactive lineflow measurements at both ends of each line.

measurement accuracy:

- 1 1% case: $\alpha = \beta = 0.01$.
- 5 5% case: $\alpha = \beta = 0.05$.

load pattern:

- F constant demand.
- S step change at $t = 180$.
- R ramp from $t = 91$ till $t = 270$.

Table 3-5: Name conventions for simulation.

These names are used in the remainder of this report.

3.5 Test quantities.

Three test quantities were chosen for comparing the three methods: The estimation error, the lineflow error and the measurement index. The estimation error is the norm of the vector difference between the estimate and the true state:

$$\text{estimation error} = \|\underline{x} - \underline{x}_{\text{true}}\| \quad (3.1)$$

This indicates how close the estimate is to the true state. From the estimate a number of quantities can be computed. A small estimation error does not have to mean a small error in the quantities computed from the estimate. Important quantities computed from the estimate are the lineflows. Therefore the lineflow error is chosen as the second test quantity. This error is defined as the norm of the vector difference between the estimated lineflows and the true lineflows:

$$\text{lineflow error} = \|\underline{g}_{\text{lf}}(\underline{x}) - \underline{g}_{\text{lf}}(\underline{x}_{\text{true}})\| \quad (3.2)$$

The last quantity, the measurement index, is defined as:

$$\text{measurement index} = \frac{\|\underline{g}(\underline{x}) - \underline{g}(\underline{x}_{\text{true}})\|}{\|\underline{y} - \underline{g}(\underline{x}_{\text{true}})\|} \quad (3.3)$$

If the estimate is good this quantity should be smaller than 1. This means that the estimated values of the measurements are better than the measurements themselves. If the measurement index is larger than 1 the measurements are better than the estimated values. Here only the measurements and their estimated values are compared, while in the lineflow error also the non measured line

flows are taken into account. The quantities computed for each simulation are summarized in the following table.

Estimation error.

Average estimation error.

Maximum estimation error at timepoint k.

Maximum element in all estimation errors at timepoint k in real (imaginary) part of busvoltage i.

Lineflow error.

Average lineflow error.

Maximum lineflow error at timepoint k.

Maximum element in all lineflow errors at timepoint k in active (reactive) flow at A(B)-end of line j.

Measurement index.

Average measurement index.

Maximum measurement index at timepoint k.

Table 3-6: The test quantities computed for each simulation.

4. The properties of the three methods.

4.1 Method A.

The first thing looked at was the convergence of method A (eq. 2.1) from a flat voltage start (all busvoltages = 1.0). Using the maximum load demand, the 2L measurement system (see table 3-5) and 1% measurements method A converged in two iterations with linearization in both iterations. In the first iteration the linearization is done around the flat voltage profile. When $G^T R^{-1} G$ was not recomputed in the second iteration divergence occurred. These results are given in table 4-1.

iter.	loss function	lin. est.	err.	loss function	lin.
0	118827.44	-	0.24	118827.44	-
1	389.91	yes	0.16	389.91	yes
2	39.74	yes	0.05	40490.08	no

Table 4-1: Flat voltage start for method A.

The loss function is defined as

$$J = \{y - g(\underline{x})\}^T R^{-1} \{y - g(\underline{x})\} \quad (4.1)$$

R^{-1} is the same diagonal weighting matrix as used in the previous chapter. In table 4-1 also the estimation error as defined by 3.1 is included. Because of these results the linearization distance Δx_1 was chosen as 0.1.

When $\|\underline{x} - \underline{x}_1\| > \Delta x_1$ a new linearization is done.

As was pointed out in the previous chapter a displacement of the linevoltage structure along the real axis (fig. 3.2 - 3.4) does not change the lineflows too much. In a measurement system with a large amount of lineflow measurements this has as a consequence that also the loss function does not change too much. Since method A tries to minimize the loss function with only the present measurements, the line voltage structure can move quite a bit along the real axis between two estimates and as a consequence a number of "unnecessary" linearizations can occur dependent on the redundancy of the measurement system (defined as number of measurements/number of state variables) and the measurement accuracy.

At each time point during a simulation first the loss function 4.1 is computed using the old estimate and the new measurements. When this is less than a critical value J^* no further action is taken. In the other case a new estimate is computed. This is called an action below. J^* is chosen as $2 \times$ number of measurements. If R really is the covariance matrix of the measurement noise J should be of the order number of measurements. In the case of method A each action can include a linearization.

Simulation	actions	linearization
A2L1F	16	2
A1L1F	108	32
A2L5F	7	6
A1L5F	129	110

Table 4-2: Actions and linearizations of method A.

Table 4-2 shows the increase of the number of linearizations when the redundancy and the measurement accuracy decreases. A linearization asks much more computing time than using a constant $G^T W G$ matrix. Nothing has been found in the literature on "unnecessary linearizations".

4.2 Method B.

The things looked at with method B (eq. 2.2) are the ordering of measurements and the choice of values for Q .

The measurement ordering is important for two reasons:

- Since the estimator uses the estimate after j measurements when processing the $j + 1$ -st one in calculating G and the residue, it is important that the estimate is already as good as possible.
- When processing the $j + 1$ -st measurement the estimator can only change the busvoltages with which the measurement has something to do (for a lineflow or line current measurement the two busvoltages at the line ends) because the used P -matrix is diagonal.

4.2.1 Tuning of ordering of measurements.

Three different orderings were tested. All three went through the networks in the following way. Starting at the reference bus first the measurements of the loop consisting of lines 11, 6 and 7 (see fig. 3.1) are taken. Then the voltage at bus 1 is determined by taking lines 4 and 2. The semiloop consisting of lines 3, 12 and 13 is processed before the heavy loaded lines 5 and 1. Finally the loose lines 8 and 10 are taken.

For testing this the LV measurement system with 1% measurements (see table 3-5) was used. The three orderings differed in:

- I When going to another bus, take first the voltage measurement (if not already used) followed by the active lineflow measurement before the reactive one.
- II The same as I but the reactive measurement before the active one.
- III The same as I but taking all ten voltage measurements at the end.

The results after 1 iteration using an initial P-matrix with all diagonal elements = 100.0 (interpretation: almost no confidence in the initial estimate) and a flat voltage profile as initial estimate are given below.

measurement ordering	I	II	III
loss function after 1 iter.	310.95	10014.90	8262.23
estimation error	0.03	0.15	0.08
lineflow error	0.52	3.38	2.32

Table 4-3: Measurement ordering for method B.

Measurement ordering I is the best of the ones investigated. Active lineflow measurements mainly determine angle differences (in rectangular coordinates imaginary parts of busvoltages, if the angular differences are small, see fig. 3.2 - 3.4) while reactive measurements determine voltage magnitudes (real parts in rectangular coordinates for small angle differences).

In I and II, when going from one bus to the next, the real parts of the two busvoltages are better determined than the imaginary parts before processing the lineflow measurements. This is because of the already processed voltage measurement, which mainly influences the real part (magnitude), and the old estimate. Therefore the next measurement should try to diminish the uncertainty in the imaginary parts. This is best done by an active flow measurement.

System III is bad because placing all the voltage measurements at the end destroys the linevoltage structure. This is shown by the estimation and lineflow error in table 4-3.

For the 2L measurement system the same ordering is used, but without the voltage measurements. The best results were obtained when processing all measurements concerned with one line directly after each other. The 1L measurement system also uses the same ordering without the voltage measurements. When using the 2L measurement system with 1% measurements it was possible to obtain converge in one iteration from a flat voltage start.

4.2.2 Tuning of Q.

The next point is the tuning of Q. Q can be interpreted as a measure of how much the estimate is allowed to change. Using the same values for all diagonal Q elements gave similar results as using values proportional to the change of each busvoltage in fig. 3.3. Comparing the results for three simulations with a ramp as load pattern and Q values of $0.4 \cdot 10^{-10}$, $0.4 \cdot 10^{-6}$ and $0.4 \cdot 10^{-5}$ respectively (see the appendix: simulations B2L1R) one sees that $0.4 \cdot 10^{-10}$ is too small, $0.4 \cdot 10^{-6}$ gives a too large lineflow error while $0.4 \cdot 10^{-5}$ produces good results. When using

a constant load values of Q , of $0.4 \cdot 10^{-10}$ and $0.4 \cdot 10^{-1}$ produced similar results.

So the choice of Q is much less critical than the choice of measurement ordering. The value of Q should be chosen large enough to give the estimator the opportunity to follow the demand. Compare e.g. the ramp and step results for method B.

4.3 Method C.

The convergence of method C (equations 2.3 - 2.5) from a flat voltage start is the only thing looked at in detail for method C. As convergence criterion is chosen

$$|\hat{x}_{i+1} - \hat{x}_i| < \epsilon \quad (4.2)$$

If ϵ is chosen too small then we may stop too early. Therefore the value of the loss function 4.1 is checked afterwards. With $\epsilon = 0.001$ method C converged in 5 iterations from a flat voltage start. In later simulations an ϵ value of 0.01 is used to speed up the convergence. During normal operation one or two iterations were sufficient. In a test example consisting of two buses and one line with low shunt admittances and a very high series impedance (precisely the opposite from the real situation) method C diverged already after the first iteration. This occurred even when using true values for the measurements. The computing noise was sufficient to cause divergence! One of the assumptions made by method C is that the line flow mainly is determined by the line current through the series impedance. This was not at all the case in the test example. An interesting point to be looked at is the performance of

method C with a network containing lines with relatively high shunt currents (long lightly loaded lines).

One of the disadvantages of method C is the direct use of the reference voltage measurement. This means that the distance of the linevoltage structure of fig. 3-2 from the origo is determined directly by the voltage measurement. For more details see the next chapter.

5. The results of the comparison.

This chapter starts with presenting the results for computing time and storage used for the three methods, followed by the results of the simulation in four tables and finally an interpretation of these results.

5.1 Computing time and storage.

Each method started at a timepoint by first computing the loss function and deciding if a new estimate should be computed (see section 4.1). After the estimate is computed it is decided if another iteration (only for method A and B) should be taken by computing the loss function based on the new estimate. The storage used by the three methods inclusive the just described administration of the loss function is given in table 5-1.

	Instructions	Data	Total
Method A	1150	3126	4276
Method B	1659	1704	3363
Method C	858	1916	2774

Table 5-1: Storage used by the three methods (decimal).

For method A the jacobian needs 732 storage places and G^{TWG} plus its decomposition 800. The storage required for G^{TWG} is proportional with n^2 (n : number of state variables) and for the jacobian proportional to m (m : number of measurements) when only the non zero elements are stored, otherwise with $m n$. For method C the matrix B^{TDB} and its decomposition use 200 places.

B^{TDB} always requires a factor 4 less storage than G^{TWG} when used for the same network since B^{TDB} can be used for both the real and imaginary parts of the busvoltages. Method B requires more instructions because of the way the sequential processing is coded. Method C requires less than A because it is simpler in set up.

The measured execution times of the estimators proper, thus without the determination of the loss function, compared with the theoretical ones estimated by counting each operation as 5 μ secs but not taking into account subroutine calls are given below.

method	A lin	A no lin	B	C(2 iter.)
measured time	128	49	54	24
estimated time	30	14	16	12

Table 5-2: Execution times in msec.

The differences between measured and estimated times can be explained by the time needed for subroutine calls, especially when containing a matrix as argument, and returns. For method A e.g. a call is done for each measurement to update the jacobian an other call to update G^{TWG} and a third one to update $G^{TW}\{y - g(x)\}$. On the Univac 1108 where the simulations were done (see /2/) such a call can take up to 100 μ secs. Because of this it was not noticed that even when there is no linearization done the already computed G^{TWG} matrix is decomposed each time a new estimate is calculated! The measured time for method A without linearization in table 5-2 is this wrong time. It is about 18 μ secs too large.

Much of this is machine dependent but one conclusion is: don't neglect the time necessary for organization. Also important when looking at computing times is the number of times the estimator is scheduled because the critical loss comes over the critical value J^* . The time needed for the administration of the loss function was 12 msec. This time is not included in the measured times of table 5-2.

5.2 The simulations.

With the possibilities mentioned in table 3-6 there are 48 simulations possible. Of these all 24 simulations using 1% measurements are done plus a number of ramp simulations using 5% measurements.

These are presented in tables 5-3 through 5-6.

In the tables the best values for each measurement system are underlined.

An interpretation of these results is given in the next section. For a more detailed presentation see the Appendix.

	average estimation error	maximum estimation error	average lineflow error	maximum lineflow error	measurement index	maximum measurement index
A2L1F	0.027	0.105 t = 83	0.114	0.170 t = 82	0.504	1.126 t = 254
ALV1F	0.023	0.092 t = 298	0.228	0.356 t = 285	0.816	1.480 t = 295
ALL1F	0.050	0.192 t = 297	0.230	0.421 t = 18	0.917	2.221 t = 295
B2L1F	<u>0.005</u>	<u>0.006</u> t = 17	<u>0.081</u>	<u>0.109</u> t = 1	<u>0.360</u>	<u>0.590</u> t = 11
BLV1F	<u>0.002</u>	<u>0.003</u> t = 312	<u>0.083</u>	<u>0.158</u> t = 312	<u>0.309</u>	<u>0.750</u> t = 300
BL11F	<u>0.004</u>	<u>0.008</u> t = 2	<u>0.100</u>	<u>0.297</u> t = 1	<u>0.422</u>	<u>0.936</u> t = 104
C2L1F	0.034	0.164 t = 188	0.115	0.202 t = 188	0.514	0.857 t = 11
C1L1F	0.062	0.208 t = 193	0.198	0.418 t = 18	0.794	1.447 t = 193

Table 5-3: Simulation results, constant load pattern, 1% measurements.

	average estimation error	maximum estimation error	average lineflow error	maximum lineflow error	measurement index	maximum measurement index
A2L1S	0.032	<u>0.066</u> t = 180	<u>0.102</u>	<u>0.168</u> t = 41	<u>0.465</u>	<u>0.965</u> t = 40
ALV1S	<u>0.023</u>	<u>0.104</u> t = 298	0.187	<u>0.368</u> t = 14	0.703	<u>1.420</u> t = 314
ALL1S	0.032	<u>0.053</u> t = 82	0.193	<u>0.374</u> t = 18	0.829	1.769 t = 213
B2L1S	<u>0.024</u>	0.101 t = 180	0.110	2.457 t = 180	0.488	10.599 t = 180
BLV1S	<u>0.023</u>	0.114 t = 180	<u>0.134</u>	3.010 t = 180	<u>0.526</u>	12.692 t = 180
B1L1S	<u>0.024</u>	0.111 t = 180	<u>0.151</u>	2.940 t = 180	<u>0.655</u>	16.133 t = 180
C2L1S	0.036	0.167 t = 51	0.128	0.195 t = 36	0.582	1.091 t = 64
CLL1S	0.062	0.209 t = 193	0.194	0.379 t = 18	0.805	<u>1.449</u> t = 193

Table 5-4: Simulation results, step load pattern, 1% measurements.

	average estimation error	maximum estimation error	average lineflow error	maximum lineflow error	measurement index	maximum measurement index
A2L1R	0.035	<u>0.171</u> t = 148	0.121	<u>0.213</u> t = 111	0.549	<u>1.175</u> t = 111
ALV1R	0.024	0.104 t = 298	0.189	0.368 t = 18	0.713	1.442 t = 191
ALL1R	0.041	0.170 t = 327	0.196	0.374 t = 18	0.844	1.890 t = 314
B2L1R	<u>0.024</u>	<u>0.042</u> t = 273	<u>0.104</u>	0.219 t = 105	<u>0.471</u>	<u>1.325</u> t = 104
BLV1R	<u>0.023</u>	<u>0.039</u> t = 271	<u>0.128</u>	<u>0.236</u> t = 105	<u>0.510</u>	<u>1.294</u> t = 104
BLL1R	<u>0.023</u>	<u>0.038</u> t = 280	<u>0.136</u>	<u>0.273</u> t = 1	<u>0.601</u>	1.694 t = 104
C2L1R	0.048	0.225 t = 204	0.131	0.214 t = 106	0.599	1.171 t = 106
C1L1R	0.062	0.208 t = 193	0.195	0.379 t = 18	0.807	<u>1.453</u> t = 193

Table 5-5: Simulation results, ramp load pattern, 1% measurements.

	average estimation error	maximum estimation error	average lineflow error	maximum lineflow error	measurement index	maximum measurement index
A2L5R	0.175	0.505 t = 268	0.607	1.074 t = 136	0.552	1.263 t = 135
A1L5R	0.243	1.037 t = 1	0.944	2.320 t = 161	0.812	1.967 t = 314
B2L5R	<u>0.031</u>	<u>0.042</u> t = 187	<u>0.475</u>	<u>0.863</u> t = 139	<u>0.429</u>	<u>0.930</u> t = 135
B1L5R	<u>0.035</u>	<u>0.051</u> t = 187	<u>0.622</u>	<u>1.327</u> t = 1	<u>0.545</u>	<u>1.528</u> t = 135
C2L5R	0.226	0.821 t = 162	0.588	0.972 t = 35	0.537	1.080 t = 166
C1L5R	0.329	1.260 t = 343	0.991	1.876 t = 18	0.849	1.557 t = 104

Table 5-6: Simulation results, ramp load pattern, 5% measurements.

5.3 Interpretation of the results.

Method B appears to be the best one. The large maximum error values in the step case are caused by the memory of the estimator (value of Q).

Both method A and C determine the line voltage structure but not the distance of this structure to zero. C is worse than A in this respect because it treats the busvoltage measurement as having the true value. When really using the true value the estimation error dropped to 0.02 in the 5% case (C1L5R) but the lineflow error stayed at 0.99. This jittering along the real axis of the line voltage structure increases the chance that J comes over J* and therefore, especially in the case of method A, increases the computational load. This can prevent the computer from doing other important tasks in a real time situation. The main cause for this jittering is the fact that methods A and C do not use the information that the state changes not very much between two timepoints. At each timepoint these methods throw away the information contained in the old estimate. This is also illustrated by the way these methods are able to follow a step.

Because method B uses both the old estimate and the new measurementset one may expect that methods A and C are able to minimize the loss function for the new measurements better than method B. This is supported by the following results:

simulation	A2L5	B2L5	C2L5	A1L5	B1L5	C1L5
loss	37.82	93.56	39.94	8.71	13.41	8.58

Table 5-7: The loss function at timepoint 0.

6. Conclusions and suggestions.

As result of this comparison of the three methods on computing time, storage used, measurement systems and measurement accuracy, using this network where the busvoltages lie relatively close together, one can say method B is the best one. The comparison does not include the effects of bias on measurements, errors in network parameters and network structure, loss of measurements and measurements in gross error. Method B is best because it exploits the knowledge of the slowly changing state better than methods A and C. However the ordering of the measurements should be done carefully. Each new measurement should diminish the uncertainty of those state variables of the ones the measurement can influence, that have the largest uncertainty.

Both method C and A do not include the old estimate in calculating the new one. They only use it for having a good start value to speed up convergence. Method C has about the same performance as method A but uses much less computing time and storage.

Since the powerflow in the network in principle is determined by the linevoltages one can say that the choice of busvoltages as state variables is doubtful. The estimators have to know the busvoltages very accurate to determine the voltage differences. The relative error of the difference of two nearly equal numbers is much larger than the relative error of the numbers themselves, but these differences are the things we want to know. A better choice might be the linevoltages of a network tree and one busvoltage.

In real time applications method B might prove to sensitive to loss of a measurement.

A few of the things that should be looked at are the inclusion of voltage measurements in method C, the possibility of averaging over a number of measurement sets with method C and the performance of the methods in a network where the bus voltages do not lie close together.

The inclusion of more voltage measurements and the averaging operation for method C might be implemented as follows. Assume first that the old estimated value of the reference voltage is correct and estimate the line voltage structure using the line flow measurements, then assume the new line voltage structure fixed and use the voltage measurements to estimate the position of this structure to zero. One can place a certain weight on the old position.

One thing that should be looked at is the sensitivity of method B to changes in the measurement system. What is the minimum set necessary for method B to give acceptable results? The results indicate that a number of voltage and line flow measurements may be lost without affecting the performance of method B too much, especially when compared with the other methods.

Also interesting for method B is the use of a block diagonal P-matrix which includes the coupling of real and imaginary parts of the bus voltages. Then the ordering may become less critical.

7. Acknowledgements.

The work reported in this and two other reports /1, 2/ is done as partial fulfillment of the requirements for the masters degree in electrical engineering at the Eindhoven University of Technology, Eindhoven, the Netherlands during the period August 1973 - April 1974 in Lund, Sweden.

I'd like to thank the Division of Automatic Control, Lund Institute of Technology, and its head professor K.J. Åström for providing the hospitality and the Swedish Institute for the scholarship for this period.

A special word of thanks to my coach in Lund Sture Lindahl who always had time to discuss problems and results and to my supervisor in Eindhoven professor dr.ir. P. Eykhoff.

8. References.

1. Van Overbeek, A.J.M.; State Estimation Methods in Power Networks I, a Literature Survey; Report 7331(C), Lund Institute of Technology, Division of Automatic Control, Lund, November 1973.
2. Van Overbeek, A.J.M.; State Estimation Methods in Power Networks III, Program Description; Report 7404(C); Lund Institute of Technology, Division of Automatic Control, Lund, April 1974.
3. Schweppe, F.C. and others; Power System Static State Estimation, Part I-III, IEEE Transactions on Power Apparatus and Systems, Vol. PAS-89, No. 1, January 1970, pp 120-135.
4. Masiello, R.D. and F.C. Schweppe; A Tracking Static State Estimator, IEEE Transactions on Power Apparatus and Systems, Vol. PAS-90, No. 3, May/June 1971, pp 1025-1033.
5. Debs, A.E. and R.E. Larson; A Dynamic Estimator for Tracking the State of a Power System, IEEE Transactions on Power Apparatus and Systems, Vol. PAS-89, No. 7, September/October 1970, pp 1670-1676.
6. Debs, A.E., R.E. Larson and L.P. Hajdu; On-Line Sequential State Estimation for Power Systems, Proceedings of the Fourth Power Systems Computation Conference, Vol. 3, Department of Electrical and Electronic Engineering, Queen Mary College, University of London, London, 1973, paper 3.3/3.

7. Dopazo, J.F., O.A. Klitin, G.W. Stagg and L.S. van Slyck; State Calculation of Power Systems from Line Flow Measurements, IEEE Transactions on Power Apparatus and Systems, Vol. PAS-89, No. 7, September/October 1970, pp 1698-1708.
8. Dopazo, J.F., O.A. Klitin and L.S. van Slyck; State Calculation of Power Systems from Line Flow Measurements, Part II, IEEE Transactions on Power Apparatus and Systems, Vol. PAS-91, No. 1, January/February 1972, pp 145-151.
9. Dopazo, J.F. O.A. Klitin, A.M. Sasson and L.S. van Slyck; Real-Time Load Flow for the AEP System; Proceedings of the Fourth Power Systems Computation Conference, Vol. 3, Department of Electrical and Electronic Engineering, Queen Mary College, University of London, London, 1973, paper 3.3/8.
10. Dopazo, J.F., S.T. Ehrmann, O.A. Klitin and A.M. Sasson; Justification of the AEP Real Time Load Flow Project, IEEE Transactions on Power Apparatus and Systems, Vol. PAS-92, No. 5, September/October 1973, pp 1501-1509.

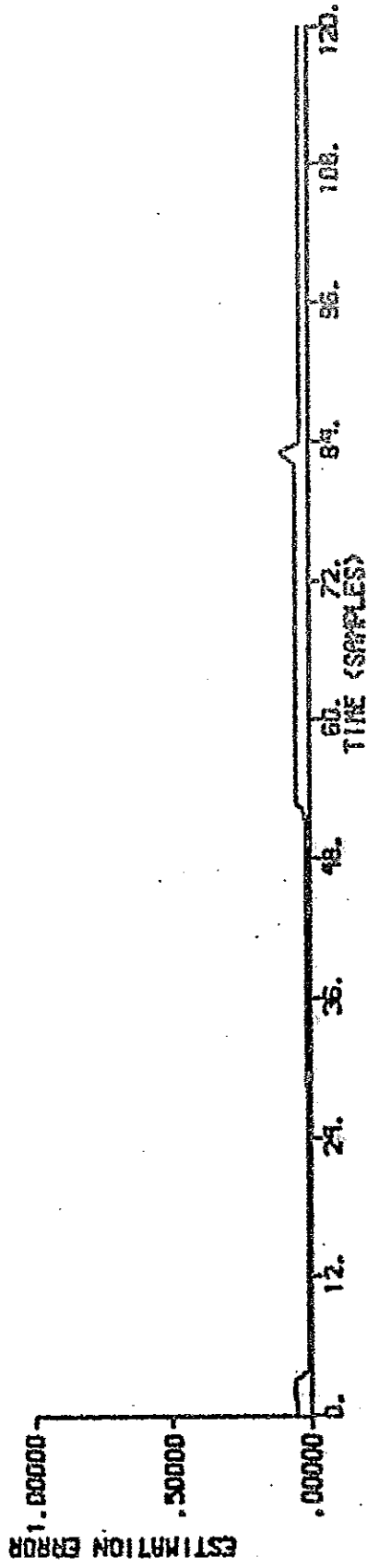
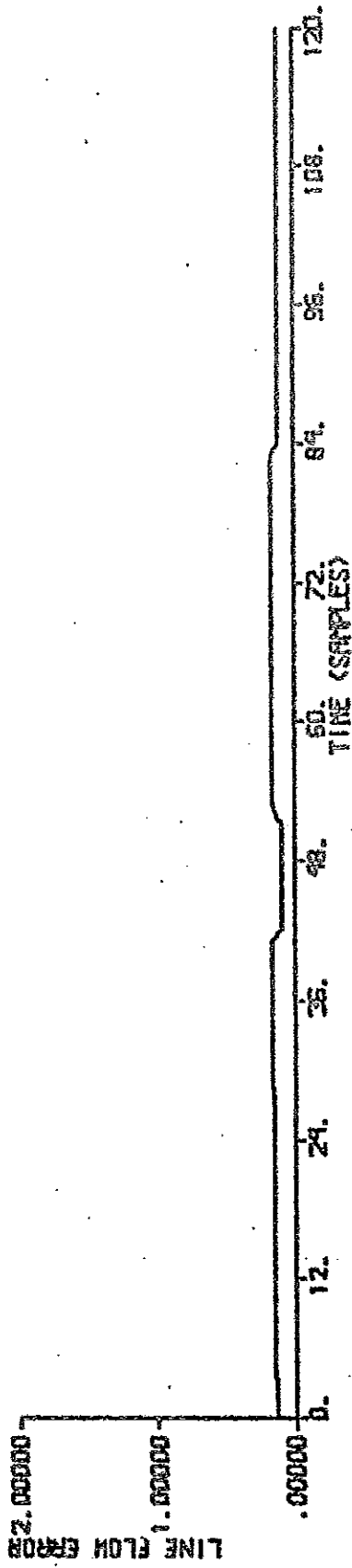
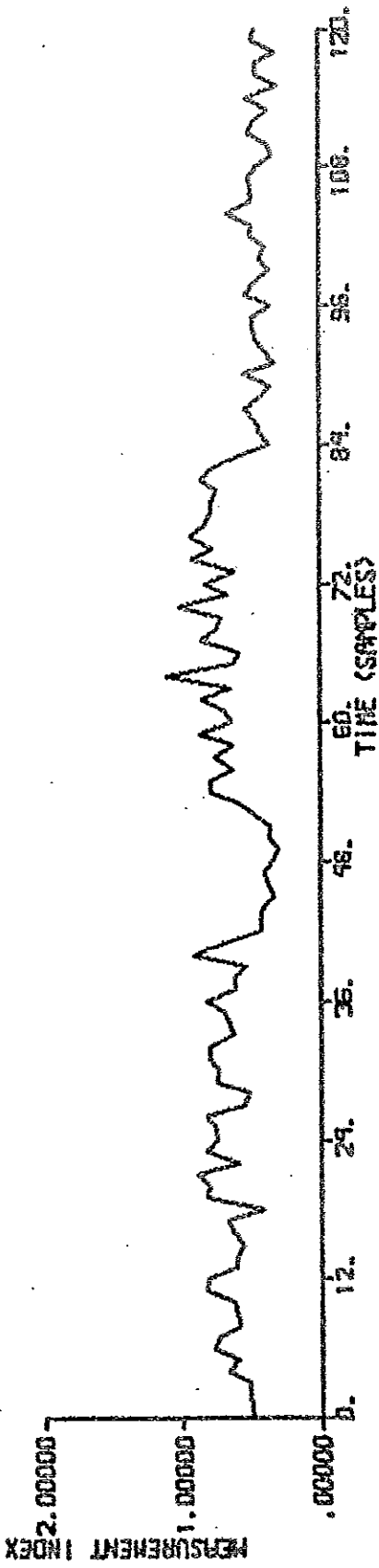
Appendix: The simulations.

This appendix contains the results of all simulations. Of each simulation are given the error quantities from table 3-6 and three plots showing the estimation error, the lineflow error and the measurement index as function of time. If nothing is said under remarks the following values are used for the critical loss J^* , the linearization distance Δx_1 , and the diagonal elements of the matrix Q of eq. 2.2 for method B:

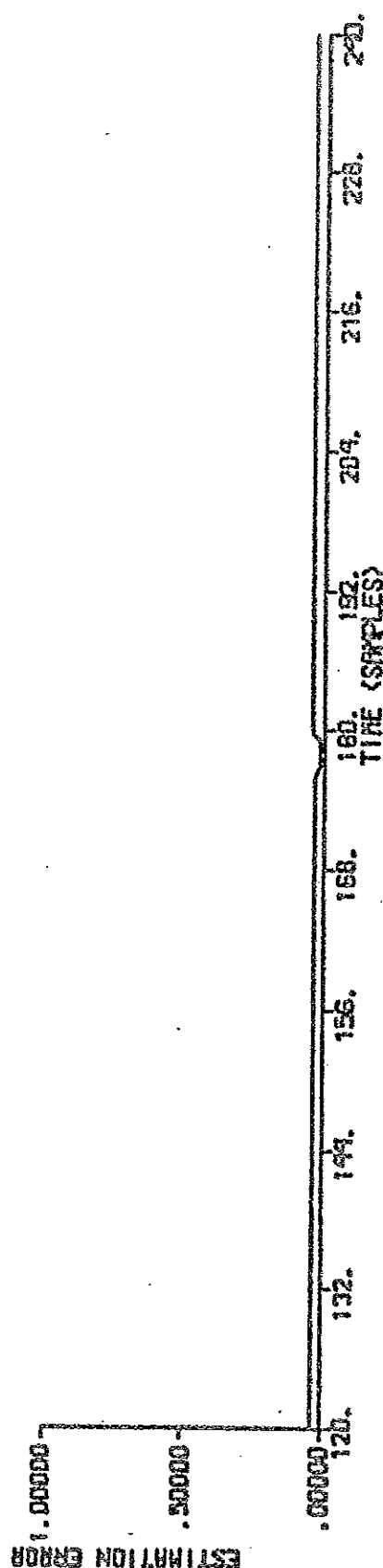
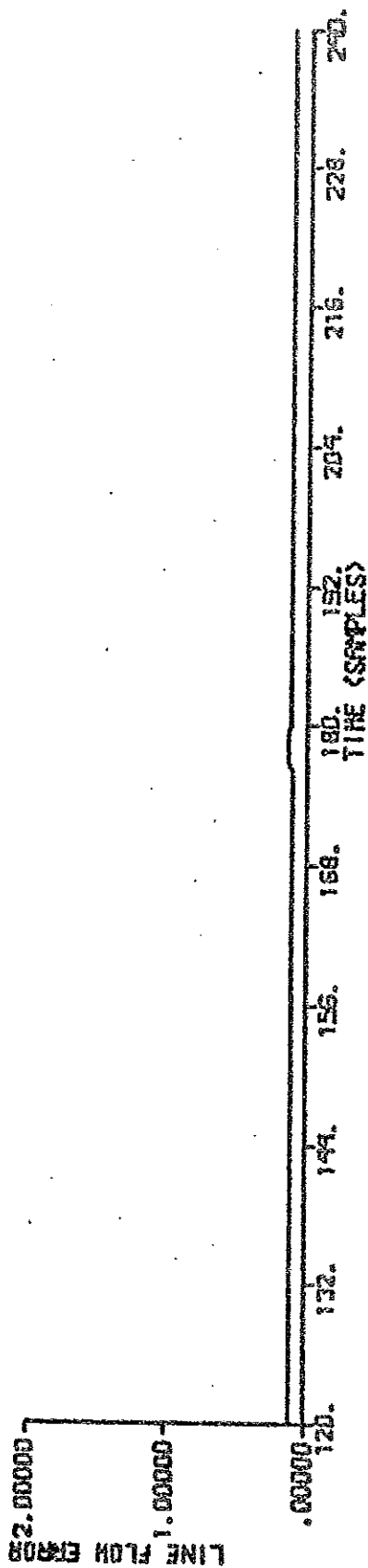
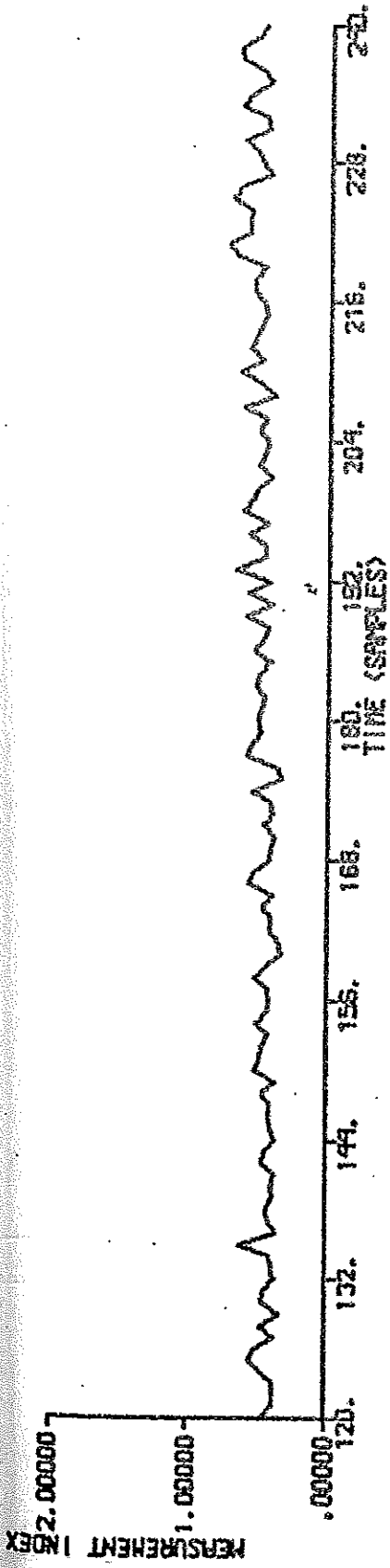
- for measurement system 2L $J^* = 106$
- for measurement system LV $J^* = 72$
- for measurement system 1L $J^* = 54$
- for method A $\Delta x_1 = 0.1$
- for method B $Q = 0.4 \cdot 10^{-5}$

Simulation	Remarks	Page
A2L1F		45
ALV1F		49
A1L1F		53
B2L1F		57
B2L1F	$Q = 0.4 \cdot 10^{-10}$	61
B2L1F	$Q = 0.4 \cdot 10^{-1}$	65
BLV1F	$J^* = 54$	69
B1L1F		73
C2L1F		77
C1L1F		81
A2L1S		85
ALV1S	$J^* = 54$	89

A1L1S		93
B2L1S		97
BLV1S	J* = 54	101
B1L1S		105
C2L1S		109
C1L1S		113
A2L1R		117
ALV1R	J* = 54	121
A1L1R		125
B2L1R	Q = 0.4 10 ⁻¹⁰	129
B2L1R	Q = 0.4 10 ⁻⁶	133
B2L1R		137
BLV1R		141
B1L1R		145
C2L1R		149
C1L1R		153
A2L5F		157
ALV5F		161
A1L5F		165
A2L5R		169
A1L5R		173
B2L5R		177
B1L5R		181
C2L5R		185
C1L5R		189



A2L1F J* = 106 $\Delta x_1 = 0.1$



A2L1F J* = 106 $\Delta x_1 = 0.1$